

## Synthetic Methods

## Cornforth–Evans Transition States in Stereocontrolled Allylboration of Epoxy Aldehydes

Robert R. A. Freund,<sup>[a]</sup> Matthias van den Borg,<sup>[b]</sup> Daniel Gaissmaier,<sup>[b, c, d]</sup> Robin Schlosser,<sup>[a]</sup> Timo Jacob,<sup>[b, c, d]</sup> and Hans-Dieter Arndt\*<sup>[a]</sup>

Dedicated to the memory of Professor Dr. Kilian Muñiz.

**Abstract:** Allylboration reactions rank among the most reliable tools in organic synthesis. Herein, we report a general synthesis of trifunctionalized allylboronates and systematic investigations of their stereocontrolled transformations with substituted aldehyde substrates, in order to efficiently access diverse, highly substituted target substrates. A peculiar transition in stereocontrol was observed from the polar Felkin–Anh (PFA) to the Cornforth–Evans (CE) model for alkoxy- and epoxy-substituted aldehydes. CE-type transition states were

uniformly identified as minima in advanced, DFT-based computational studies of allylboration reactions of epoxy aldehydes, conforming well to the experimental data, and highlighting the underestimated relevance of this model. Furthermore, a mechanism-based rationale for the substitution pattern of the epoxide was delineated that ensures high levels of stereocontrol and renders  $\alpha,\beta$ -epoxy aldehydes generally applicable substrates for target synthesis.

## Introduction

Complex natural products frequently display contiguous stereogenic substitution which contributes polarity, induces specific conformations, and allows three-dimensional branching (Figure 1). While specific biosynthesis is realized by enzymes,<sup>[1]</sup> many of these motifs are still a considerable challenge for synthesis. Prominently occurring chiral motifs in natural products are polyhydroxylated 1,2,3,4-substituted alk(en)yl carbon

chains (A, Figure 1). These are frequently found in polyketides such as the antibiotics erythromycin A and rifamycin S,<sup>[2]</sup> in terpenes such as parthenolide and micheliolide,<sup>[3]</sup> as well as in

[a] R. R. A. Freund, R. Schlosser, Prof. Dr. H.-D. Arndt  
Institut für Organische Chemie und Makromolekulare Chemie  
Friedrich-Schiller-Universität Jena  
Humboldtstr. 10, 07743 Jena (Germany)  
E-mail: hd.arndt@uni-jena.de

[b] M. van den Borg, D. Gaissmaier, Prof. Dr. T. Jacob  
Institut für Elektrochemie  
Universität Ulm  
Albert-Einstein-Allee 47, 89081 Ulm (Germany)

[c] D. Gaissmaier, Prof. Dr. T. Jacob  
Electrochemical Energy Storage  
Helmholtz-Institute Ulm (HIU)  
Helmholtzstr. 11, 89081 Ulm (Germany)

[d] D. Gaissmaier, Prof. Dr. T. Jacob  
Karlsruhe Institute of Technology (KIT)  
P.O. Box 3640  
76021 Karlsruhe (Germany)

Supporting information and the ORCID identification number(s) for the author(s) of this article can be found under:  
<https://doi.org/10.1002/chem.202001479>.

© 2020 The Authors. Published by Wiley-VCH Verlag GmbH & Co. KGaA. This is an open access article under the terms of Creative Commons Attribution NonCommercial License, which permits use, distribution and reproduction in any medium, provided the original work is properly cited and is not used for commercial purposes.

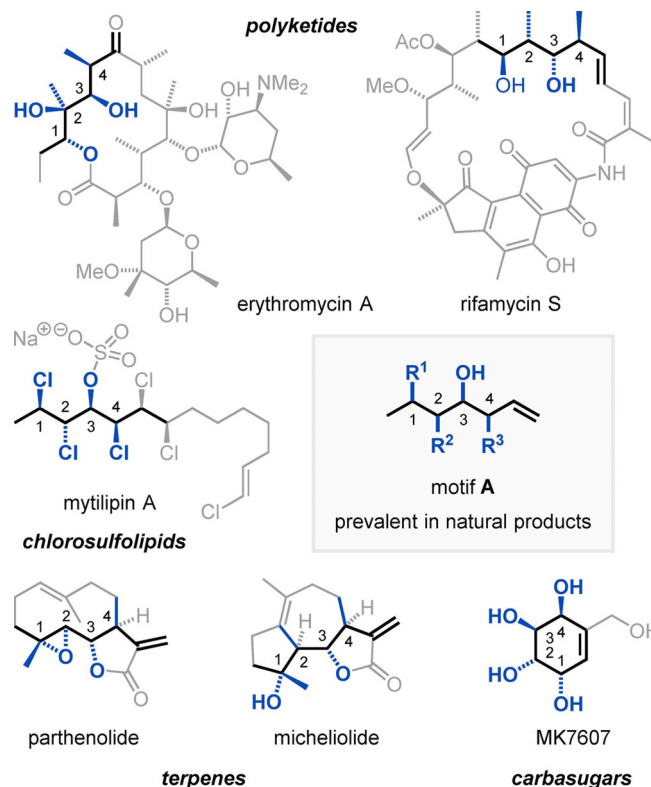
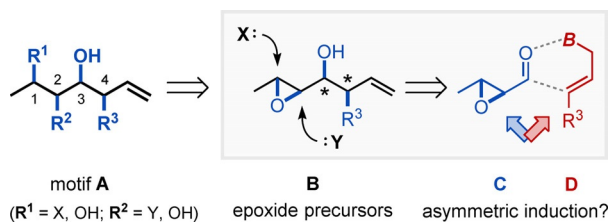


**Figure 1.** The chiral 1,2,3,4-substituted alkenyl carbon chain (A) as a prevalent motif in natural products.

carbasugars like MK7607.<sup>[4]</sup> Furthermore, such structural fragments are important synthetic building blocks, for example as synthetic precursor for the chlorosulfolipid mytilipin A.<sup>[5]</sup>

A broadly useful access to motif **A** may be provided by nucleophilic ring-opening of  $\alpha,\beta$ -epoxy alcohol **B** (Scheme 1). The

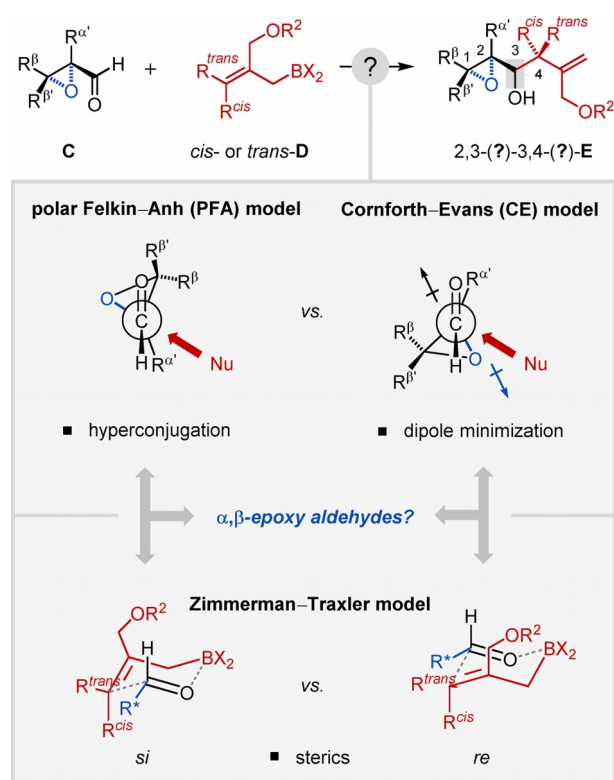


**Scheme 1.** 1,2,3,4-substituted alkenyl carbon chains accessible by allylboration.

regio- and stereochemistry of such transformations can be predictably controlled by electronic and/or steric properties of the substrate, by OH-group coordination, or by specific catalysis.<sup>[6]</sup> During work on terpene natural products we established the fragment-linking allylboration of enantioenriched<sup>[6a]</sup>  $\alpha,\beta$ -epoxy aldehydes **C** by using substituted allylboronates **D** for a direct, stereocontrolled access to  $\alpha,\beta$ -epoxy alcohols **B** (Scheme 1).<sup>[7]</sup> The configuration of the two stereogenic centers created by addition to the carbonyl group should be established by 1,2-asymmetric induction of the stereochemically-defined epoxide and the given, stable configuration of the allylboronate.<sup>[8]</sup>

However,  $\alpha,\beta$ -epoxy aldehydes (**C**) do not fit well to the common stereochemical prediction models due to the  $sp^2$  character of the  $\alpha$ - and  $\beta$ -carbon atoms and the unique geometry of the three-membered ring.<sup>[9]</sup> Therefore substrate-controlled stereoselectivity in the addition to the carbonyl group lacks general understanding with respect to direction and origin of chirality transfer (electrostatics vs. stereoelectronics) and to the influence of substitution patterns.<sup>[10]</sup> 1,2-Asymmetric induction by an  $\alpha$ -heteroatom substituent ( $C_{\alpha}$ -X) is typically rationalized by the polar variant of the Felkin–Anh–Eisenstein model (polar Felkin–Anh, PFA).<sup>[8b,11]</sup> This model favors a transition state (TS) which is stabilized by hyperconjugation, that is, a favorable interaction of the nucleophile's filled non-bonding orbital ( $n_{Nu}$ ) with the mixed empty  $\pi^*_{C=O}$  and  $\sigma^*_{C-O}$  acceptor orbitals (Scheme 2). Additional consideration of the Bürgi–Dunitz trajectory for productive overlap ( $\alpha_{BD} = 105 \pm 5^\circ$ )<sup>[12]</sup> leads to a transition state with an O=C-C-O dihedral angle of  $\theta = 75 \pm 5^\circ$  and  $285 \pm 5^\circ$ , from where nucleophilic addition occurs from the sterically less encumbered side.<sup>[11]</sup> Additions to carbonyl compounds featuring moderately electronegative groups in the  $\alpha$  position, such as  $NR_2$ ,  $SR$ , or  $PR_2$ , were shown to be under PFA control.<sup>[13]</sup>

Alternatively, the Cornforth–Evans (CE) model may operate in case of strongly electronegative substituents in the  $\alpha$ -position.<sup>[13,14]</sup> In this model, dipole moment minimization outweighs hyperconjugation, leading to an antiperiplanar orientation of the C=O and  $C_{\alpha}$ -O bond vectors in the transition state (Scheme 2). This arrangement fits to two possible ground state



**Scheme 2.** Stereocontrolled allylboration of  $\alpha,\beta$ -epoxy aldehydes: polar Felkin–Anh or Cornforth–Evans control in the context of cyclic, quasi-neutral transition states.<sup>[8b,13,14b,17]</sup>

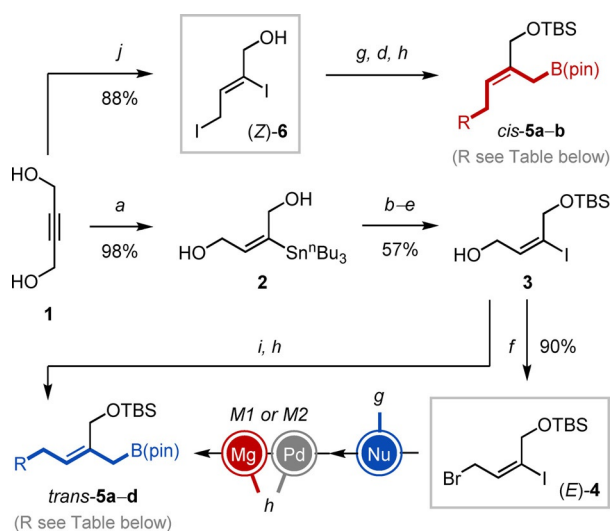
(GS) conformations displaying a dihedral angle of  $\theta_{GS} = 165 \pm 15^\circ$  and  $195 \pm 15^\circ$ , covering “late” (product-like) to “early” (substrate-like) TS geometries.<sup>[14b,15]</sup> The *re* and *si* face of the carbonyl group is then discriminated by minimizing steric interactions with the approaching nucleophile.




While both models are clearly different, their dichotomy may easily go unnoticed because for simple nucleophiles, both the PFA and the CE model predict the same product **E** (Scheme 2).<sup>[13]</sup> As the nucleophile becomes more complex, energetically distinguishable TSs, namely CE, *anti*-CE, PFA, and *anti*-PFA, may potentially lead to different reaction outcomes.<sup>[13,14]</sup> This could especially be the case for allylboration reactions that traverse a six-membered ring TS of the adapted Zimmerman–Traxler model.<sup>[16]</sup>

We therefore investigated the allylboration of  $\alpha,\beta$ -epoxy aldehydes experimentally and computationally for generating a mechanistic rationale, and for making this transformation accessible to synthesis planning also for more complex boronate nucleophiles. To meet the general acid sensitivity of epoxy aldehydes we explored reactive, functionalized 2-(silyloxymethyl)allylboronates, recently introduced as an effective tool for the formation of biologically important  $\alpha$ -*exo*-methylene  $\gamma$ -butyrolactones in the total synthesis of (–)-parthenolide.<sup>[7]</sup>

## Results and Discussion

Initially, a general *cis*- and *trans*-selective synthesis of 2-(silyloxymethyl)allylboronates from commercially available 2-butyne-



entry	boronate	R- (step: yield)	yield step h (method) boronate formation
1	<i>trans</i> -5a	 (g: 96%)	56% (M1); 50% (M2)
2	<i>trans</i> -5b	PhS- (g: 96%)	19% (M1); 40–66% (M2)
3	<i>trans</i> -5c	(2-Naph)S- (g: 97%)	0% (M1); 22% (M2)
4	<i>trans</i> -5d	 (g: 94%)	69% (M1); 54% (M2)
5	<i>trans</i> -5e	MeO-CH <sub>2</sub> -O- (i: 85%)	0% (M1 or M2)
6	<i>cis</i> -5a	 (g)	84% (M2, over 2 steps)
7	<i>cis</i> -5b	PhS- (g: 76%)	64% (M2)

**Scheme 3.** Stereoselective synthesis of *trans*- and *cis*-2-(silyloxymethyl)allylboronates. Reagents and conditions: (a) [Pd(PPh<sub>3</sub>)<sub>4</sub>] (1 mol%), *n*Bu<sub>3</sub>SnH, THF, 0 °C, 2 h, 98%; (b) Ac<sub>2</sub>O, Et<sub>3</sub>N, CH<sub>2</sub>Cl<sub>2</sub>, 5 °C, 24 h, 68%; (c) I<sub>2</sub>, CH<sub>2</sub>Cl<sub>2</sub>, -78 °C, 3 h, 92%; (d) TBSCl, imidazole, 0 °C to rt, 3 h; (e) K<sub>2</sub>CO<sub>3</sub>, MeOH, 0 °C to rt, 2 h, 83% (2 steps); (f) NBS, PPh<sub>3</sub>, CH<sub>2</sub>Cl<sub>2</sub>, -40 °C, 3 h, 90%; (g) (5a): 4 or 6, allylMgBr, THF, -40 °C, 2 h; (5b): PhSH, NaOMe, MeOH, -20 °C, 10 min, then 4 or 6, -20 to 0 °C, 3 h; (5c): (2-Naph)SH, NaOMe, MeOH, 0 °C, 30 min, then 4, 0 °C, 5 h; (5d): methallylMgBr, THF, -40 °C, 2 h; (h) method M1: *t*BuLi [or *n*BuLi (5c)], Et<sub>2</sub>O, -78 °C, 2 h, then MgBr<sub>2</sub>·OEt<sub>2</sub>, -78 °C, 1 h, then ICH<sub>2</sub>B(pin), -78 to -20 °C, 15 h; method M2: IZnCH<sub>2</sub>B(pin), [Pd(PPh<sub>3</sub>)<sub>4</sub>] (10 mol%), THF, 60 °C, 2 h; (i) (5e): MeOCH<sub>2</sub>Cl, *i*Pr<sub>2</sub>NEt, CH<sub>2</sub>Cl<sub>2</sub>, 0 °C to rt, 18 h; (j) Me<sub>3</sub>SiCl, NaI, MeCN, rt, 10 min, then 1, 1 h, 88%. Note: The *cis*-configured allylboronate has nominally (*E*) configuration [*trans* applies to (*Z*)].

1,4-diol (1) was developed (Scheme 3). The precursor for the *trans*-configured boronates, iodoallyl bromide (*E*)-4, was accessed in 50% yield over six steps via stannyldiol 2 and vinyl iodide 3,<sup>[7]</sup> allowing to introduce diverse side chains (Scheme 3, bottom). Allyl (Table in Scheme 3, entry 1) and methallyl groups (entry 4) were connected to bromide 4 by using Grignard reagents. Phenyl- and 2-naphthyl thioethers (entry 2, 3) were formed by substitution with thiolate, all with high reliability in excellent yield. Additionally, a methoxymethyl ether side chain (entry 5) was introduced by direct functionalization of alcohol 3.

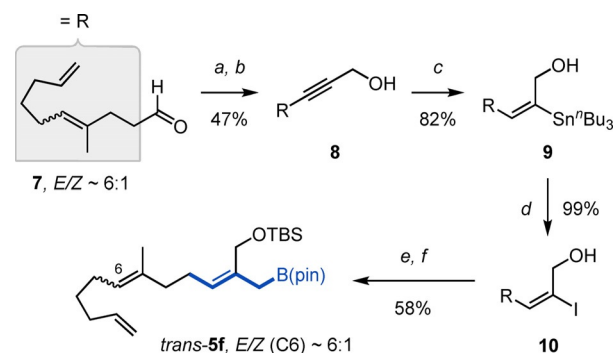
For the transformation of the vinyl iodides into allylboronates, a cascade of (I) I→Li exchange, (II) Li→Mg transmetalation<sup>[14e]</sup> and (III) trapping with ICH<sub>2</sub>B(pin) was investigated (method M1).<sup>[14e]</sup> Electron poor substrates with all-carbon side chains were smoothly transformed into allylboronates in satisfying yields (entry 1, 4). Unfortunately, in case of the more elec-

tron rich thioethers (5b and 5c) only minor amounts of the allylboronate were obtained. The major product was an allene (SI-12), probably formed via a β-elimination pathway of the electron rich intermediate.<sup>[18]</sup> Attempts to obtain the more stable vinyl magnesium reagent directly by I→MgX exchange utilizing different reactive organomagnesium compounds (*i*PrMgCl·LiCl,<sup>[19]</sup> *i*Pr<sub>2</sub>Mg·LiCl,<sup>[20]</sup> *i*Pr(*n*Bu)<sub>2</sub>MgLi·LiCl<sup>[21]</sup>) were unproductive even at elevated temperatures.

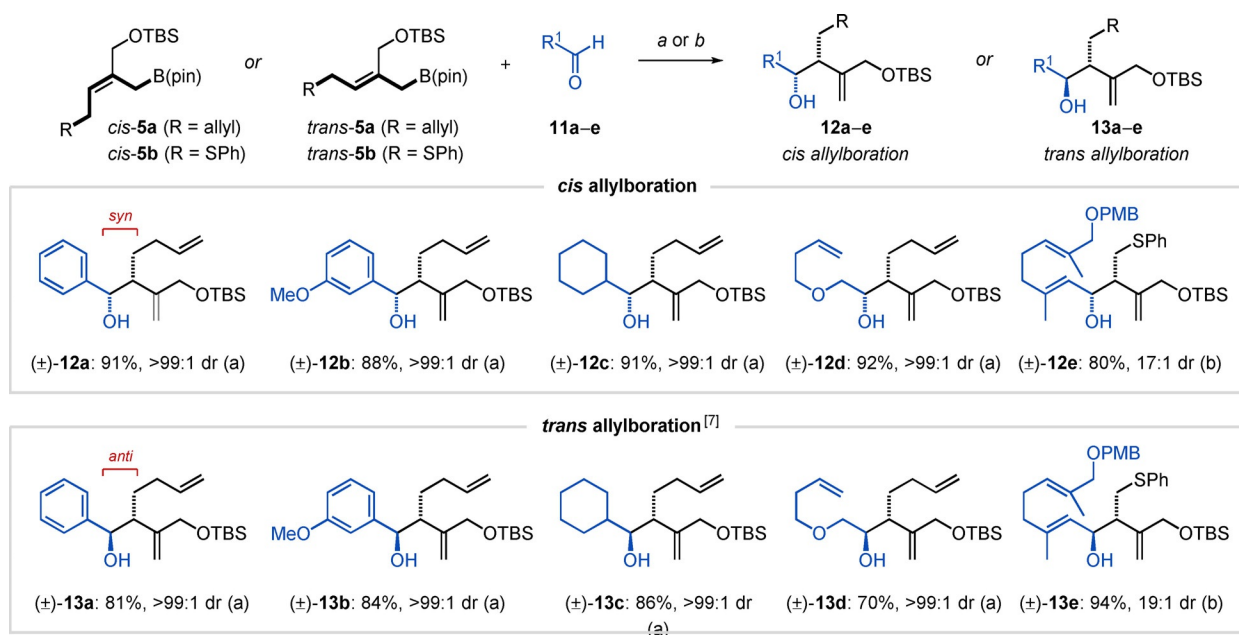
A more general way of stereoselective allylboronate formation was realized by coupling the vinyl iodides under Negishi conditions with Knochel's IZnCH<sub>2</sub>B(pin) reagent,<sup>[22]</sup> giving reproducible yields for boronates *trans*-5 including also those which contained the challenging phenyl thioether substituent (method M2, entry 1–2, 4). Unfortunately, the presence of the 2-naphthyl sulfide or an alkoxide (entry 3, 5) limited the method, probably by competing π-allyl Pd-mediated pathways or catalyst deactivation.

The corresponding reagent for the preparation of *cis*-configured boronates was obtained by Me<sub>3</sub>SiI-mediated *trans*-selective hydroiodination of 1 with simultaneous O→I exchange (Scheme 3, top), giving stable diiodide (*Z*)-6.<sup>[23]</sup> Carbon- and sulfur-based side chains were smoothly introduced by nucleophilic substitution. After *O*-silylation, allylboronates were formed by Negishi coupling, providing the boronates *cis*-5a and -5b (entry 6, 7).

Boronates with more complex side chains cannot be prepared from configurationally unstable<sup>[24]</sup> allyl nucleophiles that show [1,3]-metallotropic shifts,<sup>[8e]</sup> such as used for the synthesis of 5a and 5b. However, any ω-substituted propargyl alcohol should be a suitable substrate for allylboronate synthesis as described above (Scheme 4). As an example, the known aldehyde 7<sup>[25]</sup> was transformed into propargyl alcohol 8 by applying a Corey–Fuchs sequence, hydroxyl-directed hydrostannylation (9), and Sn→I exchange to obtain vinyl iodide 10. The latter was *O*-silylated, subjected to I→Li exchange, and trapped by ICH<sub>2</sub>B(pin) to provide the complex allylboronate *trans*-5f in good yield, suitable for installing relay alkene meta-



**Scheme 4.** Synthesis of complex boronate *trans*-5f using hydroxyl directed hydrostannylation. Reagents and conditions: (a) CBr<sub>4</sub>, PPh<sub>3</sub>, CH<sub>2</sub>Cl<sub>2</sub>, 0 °C, 1.5 h, 74%; (b) *n*BuLi, THF, -78 °C, 1 h, then (CH<sub>2</sub>O)<sub>*n*</sub>, -10 °C to rt, 3 h, 64%; (c) [PdCl<sub>2</sub>(PPh<sub>3</sub>)<sub>2</sub>] (5 mol %), *n*Bu<sub>3</sub>SnH, PhMe, rt, 1.5 h, 82%; (d) I<sub>2</sub>, CH<sub>2</sub>Cl<sub>2</sub>, -78 °C, 3 h, 99%; (e) TBSCl, imidazole, CH<sub>2</sub>Cl<sub>2</sub>, 0 °C, 30 min, 94%; (f) *t*BuLi, Et<sub>2</sub>O, -78 °C, 1 h, then ICH<sub>2</sub>B(pin), -78 to -20 °C, 15 h, 62% (modified method M1).



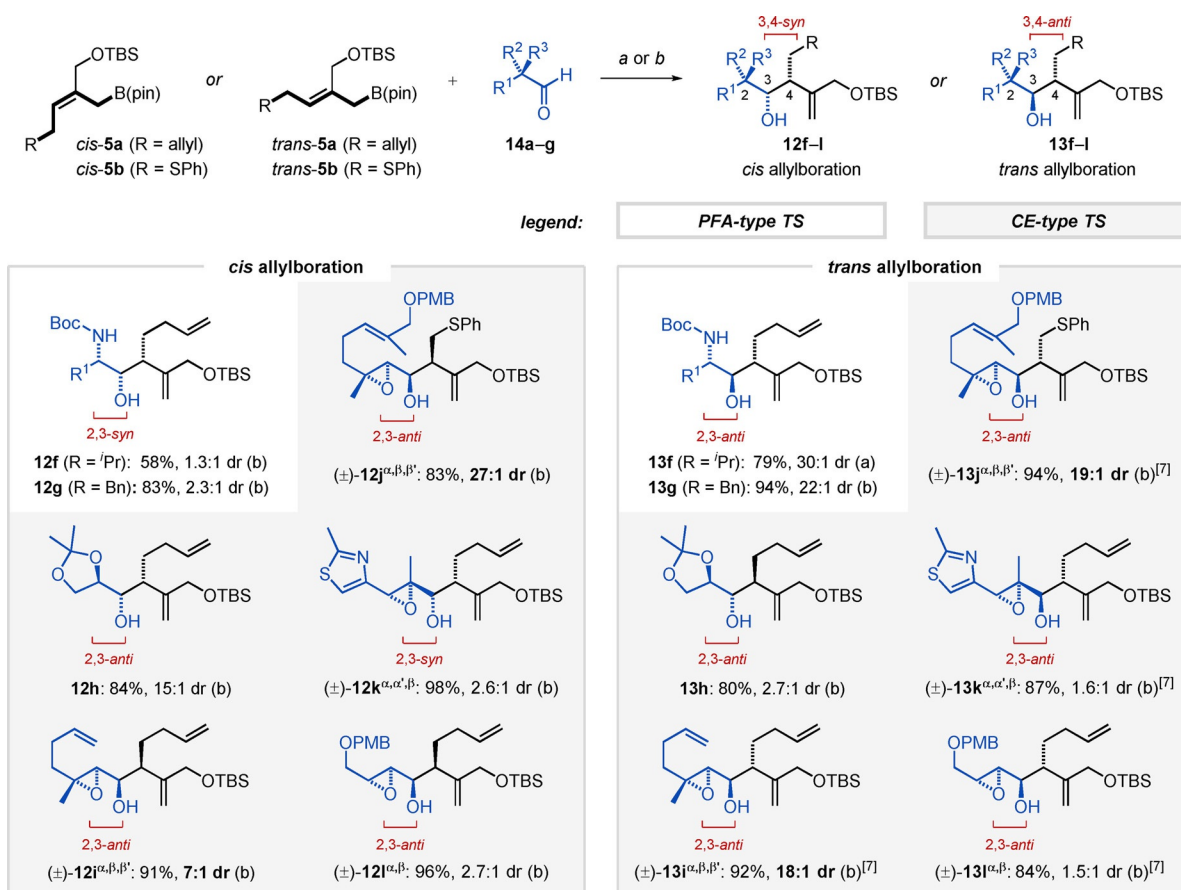
**Scheme 5.** 2-(Silyloxymethyl)allylboration of achiral aldehydes. Conditions: *cis*- or *trans*-5 (1.0 equiv), aldehyde (1.1–1.5 equiv), Et<sub>2</sub>O (0.2 M); (a) 0 to 25 °C, 24 h; (b) NaHCO<sub>3</sub> (0.05 equiv), 0–5 °C, 48 h. Combined yields are given, major isomer depicted. d.r. determined by GC-MS, HPLC, or NMR.

The reactivity of *cis*- and *trans*-2-(silyloxymethyl)allylboronates toward simple, achiral aldehydes (**11a–e**, for structures see Figure SI-1) was investigated next. Gratifyingly, smooth allylboration was already observed at 0 °C and without external activation by acids, often needed for related allylation by other allylboronates, making those novel reagents compatible with acid-sensitive substrates (Scheme 5).<sup>[27]</sup> The homoallyl alcohol products featuring aryl (**12a–b**, **13a,b**), alkyl (**12c**, **13c**), and alkoxy side chains (**12d**, **13d**) were efficiently formed under mild conditions (70–92% yield, 0 to 25 °C) for both the *cis* and the *trans* series. The products were obtained as single diastereomers, indicating complete translation of the defined boronate stereochemistry into the product according to the Zimmerman–Traxler model.<sup>[8b,17]</sup> The allylboration of a very sensitive  $\alpha,\beta$ -unsaturated aldehyde was buffered by solid NaHCO<sub>3</sub> and kept at lower temperature (0–5 °C, 48 h) to obtain the products **12e** and **13e** in good yield (80–94%) and excellent diastereoselectivity (17–19:1 d.r.).

With optimized reaction conditions in hand, the study was extended to chiral aldehyde substrates **14a–g** (for structures see Figure SI-1) featuring an  $\alpha$ -heteroatom substituent (Scheme 6). The *trans* allylboration of  $\alpha$ -carbamato aldehydes enabled the preparation of homoallyl alcohols **13f,g** with high yields (79–94%), excellent d.r.'s (22–30:1), and without detectable epimerization. In contrast, *cis* allylboration of these substrates resulted in slightly lower yields (58–83%) and low d.r. (1.3–2.3:1) of the products **12f,g**. Surprisingly, extension to an  $\alpha,\beta$ -substituted dialkoxy aldehyde reversed the trend, leading to good yield and stereocontrol for the *cis* variant (**12h**, 15:1 d.r.) while the *trans* allylboration lacked diastereocontrol (**13h**, 2.7:1 d.r.). Related findings have been sporadically reported. Dipole effects were invoked as a possible cause for the eroding stereocontrol in these cases.<sup>[28]</sup>

The stereochemistry of the  $\alpha$ -aminoalcohol carbamates **12f** and **13f** was elucidated after cyclization to the corresponding five-membered oxazolidinones which enabled their stereochemical assignment by determining their <sup>3</sup>J<sub>4H,5H</sub> coupling constants (Scheme SI-1).<sup>[29]</sup> Homoallyl alcohol **12f**, obtained as a separable 1.3:1 diastereomeric mixture, allowed for the assignment of both isomers, namely the major one as the 2,3-*syn*-3,4-*syn* product (*anti*-PFA TS) and the minor one as the 2,3-*anti*-3,4-*syn* product (PFA TS). Similarly, *trans* allylboration product **13f** (22:1 d.r.) was assigned as the 2,3-*anti*-3,4-*anti* product (PFA TS). These findings conform to the common model of PFA-type attack on the aldehyde carbonyl (cmp. to Scheme 7).<sup>[8b]</sup> In contrast, the stereoselective *cis* allylboration leading to dialkoxy alcohol (+)-**12h** was found to be either under PFA or CE control by analysis of its (*R*)- and (*S*)-Mosher esters disclosing a 2,3-*anti*-3,4-*syn* configuration (Figure SI-2).<sup>[30]</sup> Since *anti*-PFA control would be expected for *cis*-allylboration, the CE model could be relevant for the reaction of substrates with strongly electronegative  $\alpha$ -substituents.<sup>[13,14]</sup>

Different epoxide substitution patterns were studied for their impact on the asymmetric induction, including  $\alpha,\beta,\beta'$ ,  $\alpha,\alpha',\beta$ , and  $\alpha,\beta$ -*trans* substitution (Scheme 6). Gratifyingly, epoxy aldehydes featuring  $\alpha,\beta,\beta'$  trisubstitution lead to high diastereoselectivity in the *cis* case, enabling the synthesis of homoallyl alcohols **12i** <sup>$\alpha,\beta,\beta'$</sup>  and **12j** <sup>$\alpha,\beta,\beta'$</sup>  in excellent yields (91% and 83%) and d.r.'s (7:1 and 27:1). The same applied to *trans* allylboration of these  $\alpha,\beta,\beta'$  trisubstituted substrates resulting in products **13i** <sup>$\alpha,\beta,\beta'$</sup>  with d.r.'s of  $\approx$ 18:1 and high yields of 92% and 94%, respectively. However, changing the epoxide's substitution pattern from  $\alpha,\beta,\beta'$  to  $\alpha,\alpha',\beta$  tri- (**12k** <sup>$\alpha,\alpha',\beta$</sup> , **13k** <sup>$\alpha,\alpha',\beta$</sup> ) or  $\alpha,\beta$ -*trans* disubstitution (**12l** <sup>$\alpha,\beta$</sup> , **13l** <sup>$\alpha,\beta$</sup> ) resulted in loss of asymmetric induction for both the *cis*- and *trans*-configured reagents, although combined yields remained high (84–98%).



**Scheme 6.** 2-(Silyloxymethyl)allylboration of chiral  $\alpha$ -heteroatom-substituted aldehydes. Conditions: *cis*- or *trans*-5 (1.0 equiv), aldehyde (1.1–1.5 equiv), Et<sub>2</sub>O (0.2 M); (a) 0 to 25 °C, 24 h; (b) NaHCO<sub>3</sub> (0.05 equiv), 0–5 °C, 48 h. Combined yields are given, major isomer being depicted. d.r. determined by GC-MS, HPLC, or NMR.

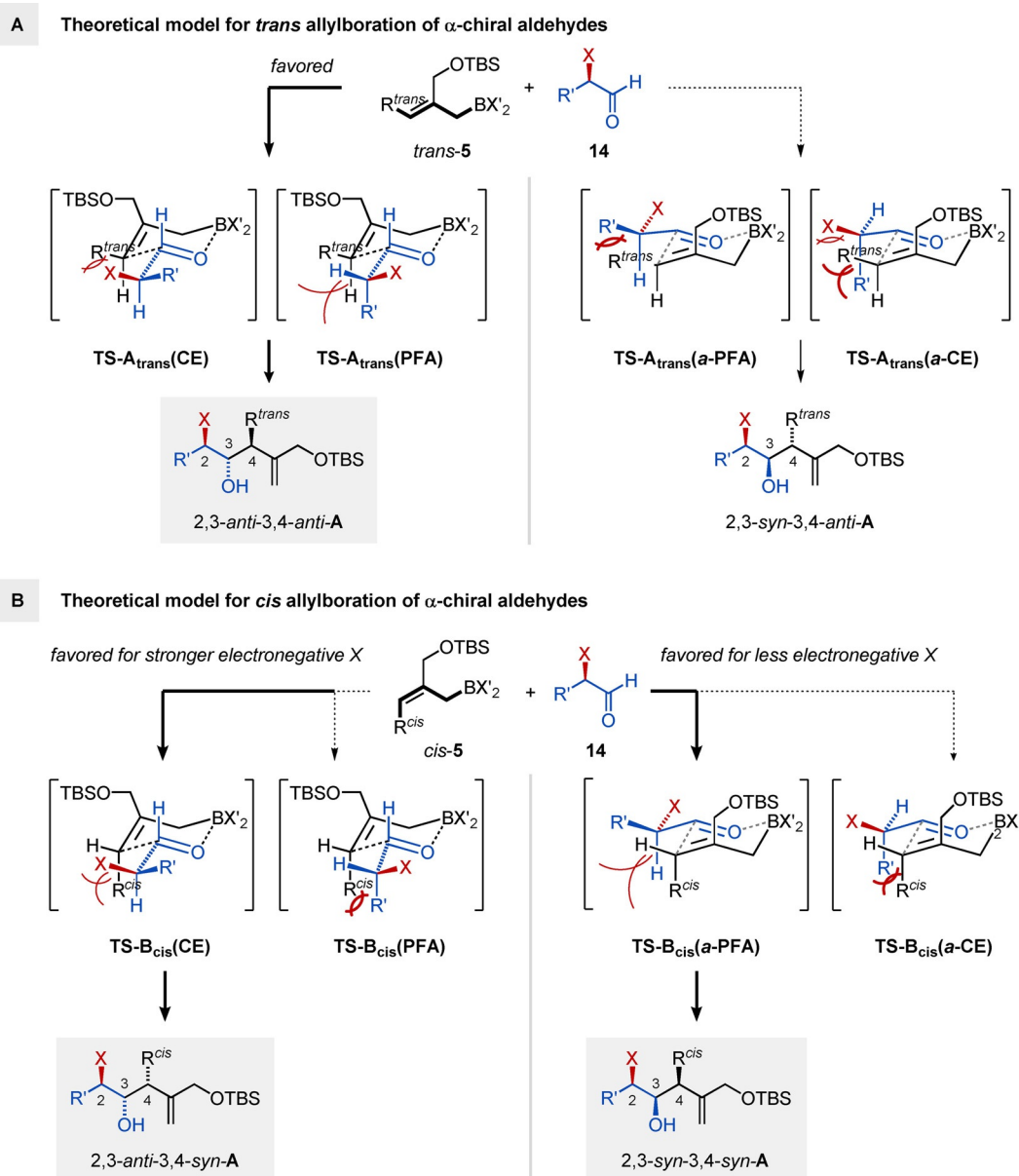
This strong effect of a *cis*- $\beta$  substituent indicated 1,3- rather than 1,2-asymmetric induction to cause the high diastereoselection.<sup>[31]</sup>

The stereochemistry of the enantiomerically-enriched epoxide-containing products (+)-**12j**<sup>α,β,β'</sup> and (+)-**13j**<sup>α,β,β'</sup> was again assigned by analyzing their Mosher esters (Figure SI-2).<sup>[30]</sup> The relative stereochemistry of both carbinols featured 2,3-*anti* configuration, even though being individually prepared from *cis* and *trans* allylboration. Since these data would correspond to either PFA or CE control in both cases (cmp. to Scheme 7), as was also found for the dialkoxy-containing substrate, dipole effects might be involved in the allylboration of epoxy aldehydes. The stereochemistry was independently validated by NMR and X-ray crystal structure analyses of the alcohols (±)-**13i**<sup>α,β,β'</sup> and (±)-**13j**<sup>α,β,β'</sup> after derivatization.<sup>[7]</sup> Interestingly, the presence of a second  $\alpha$ -substituent (R<sup>α'</sup>) decreased the directing influence of the epoxy group leading to a switch in stereochemistry from 2,3-*anti* to *syn* in case of *cis* allylboration product **12k**<sup>α,α',β</sup>.

In order to convert the flexible 2-(hydroxyethyl)-allyl alcohols into more rigid, ring-closed lactones, an efficient two-step procedure for the transformation of homoallylic substrates **12** and **13** into also more biologically relevant<sup>[32]</sup>  $\alpha$ -*exo*-methylene  $\gamma$ -butyrolactones was established (Scheme 8). Fluoride-mediated

silyl ether cleavage released a diol which was oxidatively lactonized by PhI(OAc)<sub>2</sub> and catalytic TEMPO (step b),<sup>[7,33]</sup> or equally effectively by using catalytic TPAP and NMO (step c).<sup>[34]</sup> Thereby, aryl (**15 a**, **16 a**) and alkyl substituted substrates (**15 b**, **16 b**) were converted into the corresponding lactones in high yields, as well as vinyl substituted molecules featuring an oxidation labile thioether (**15 c**, **16 c**). In addition, substrates derived from  $\alpha$ -heteroatom substituted aldehydes were smoothly transformed, showing that secondary carbamates (**15 d**, **16 d**), an acetal (**15 e**), and epoxides (**15 f**, **16 f**) were well tolerated. Unfortunately, attempts to acquire more structural information from these derivatives by NMR or X-ray crystallography was met with little success.

Therefore, in order to generate further insight, theoretical modelling was pursued by using computational methods. The reaction of *trans* allylboration with  $\alpha$ -chiral aldehydes most often results in 2,3-*anti* stereochemistry.<sup>[8b]</sup> This outcome can be explained by the common (P)FA model and was found also to match the *trans* allylboration of  $\alpha,\beta$ -epoxy aldehydes, leading for example, to product **13j**<sup>α,β,β'</sup>. On the other hand, the model suggests *anti*-PFA stereochemistry (2,3-*syn*) for *cis*-configured allylboration reagents. As 2,3-*anti* stereochemistry was found for the polar *cis* allylboration products **12h** and **12j**<sup>α,β,β'</sup>, dipole-minimized CE transition states could rather account for



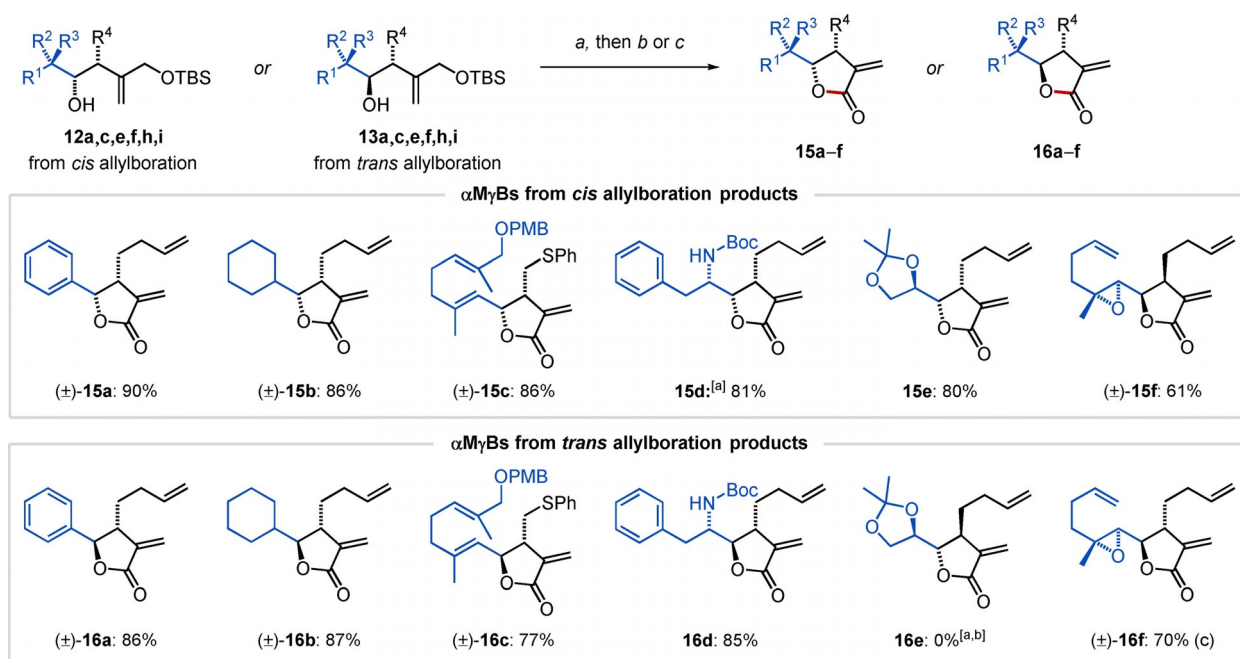
**Scheme 7.** The general Cornforth–Evans and the (polar) Felkin–Anh model for allylboration of  $\alpha$ -chiral aldehydes: Stereochemical outcome of *cis* allylboration should depend on the electronegativity of the  $\alpha$ -carbon substituent. (The atom count of product A corresponds to the one used in Scheme 2).<sup>[8b, 13, 14b,d, 16b,c]</sup>

stereochemical control.<sup>[8b, 17]</sup> In order to scrutinize this issue, DFT calculations were initiated for elucidating (1) the parameters of stereocontrol, (2) the importance of the epoxide substitution pattern, and (3) the relevance of dipole-minimized CE pathways for the allylboration of epoxy aldehydes in general.

Initially ground state (subscript GS) rotational energy profiles were calculated for  $\alpha,\beta$ -epoxy aldehyde substrates, in order to gain insight into preferred and destabilized conformations. Since allylboration traverses an “early”, substrate-like transition state regarding the C–C bond to be formed,<sup>[35]</sup> the aldehyde’s conformational preferences should be reflected in the transition state structures as well.<sup>[13, 14]</sup> For the calculation, the O=C–C–O dihedral angle  $\theta_{GS}$  of simplified substrates **17** <sup>$\alpha,\beta,\beta'$</sup> , **18** <sup>$\alpha,\alpha',\beta$</sup> , and **19** <sup>$\alpha,\beta$</sup>  featuring the substitution patterns of interest (see superscript) was incrementally varied from  $\theta_{GS}=0$  to  $360^\circ$ , fol-

lowed by geometry optimization for each step at the dispersion-corrected B3LYP-D3(BJ)/cc-pVDZ level of theory<sup>[36]</sup> in the gas phase (Figure 2).

The rotational profiles found displayed a strong conformational minimum for all three epoxy aldehydes at a dihedral angle  $\theta_{GS}$  close to  $160^\circ$ , representing a *gauche/anti* conformation that almost coincides with a minimized dipole moment by antiperiplanar orientation of the carbonyl group and the epoxide’s C–O bond.<sup>[14a]</sup> Moving the  $R_{\alpha'}$  substituent out of an eclipsed conformation as well as residual stabilizing hyperconjugative interactions with the carbonyl group probably lead to the deviation from a  $\theta_{GS}=180^\circ$  minimum.<sup>[14a, 37]</sup> Orientations of  $\theta_{GS}=75 \pm 5^\circ$  and  $285 \pm 5^\circ$  ( $-75 \pm 5^\circ$ ), which would correspond to (*anti*)-PFA TSs, were considerably disfavored by around 6–7 and 3–4 kcal mol<sup>-1</sup>, respectively. Repelling interactions with the



**Scheme 8.** Synthesis of  $\alpha$ -*exo*-methylene  $\gamma$ -butyrolactones from allylboration products. Reagents and conditions (isol. yields over 2 steps): (a) TBAF·3H<sub>2</sub>O, THF, 0 °C, 1 h; (b) TEMPO (30 mol%), Ph(OAc)<sub>2</sub>, rt, 18 h; (c) <sup>n</sup>Pr<sub>4</sub>NRuO<sub>4</sub> (TPAP, 10 mol %), NMO, 4 Å molecular sieves, CH<sub>2</sub>Cl<sub>2</sub>/MeCN (5:1), rt, 18 h. [a] Major isomer (depicted) used. [b] Decomposition during purification on silica.

residues at C- $\alpha$  or C- $\beta$  and unfavorable bond dipole orientations likely destabilize these conformations.

The obtained rotational energy profiles resemble those reported for aldehydes bearing an  $\alpha$  substituent based on a  $sp^3$ -

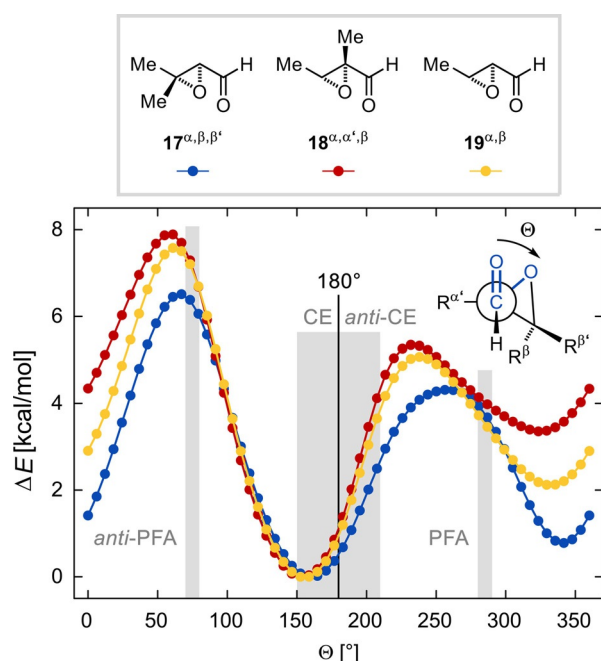


**Figure 2.** Computed rotational energy profile of simplified  $\alpha,\beta$ -epoxy aldehydes. Level of theory: B3LYP-D3(BJ)/cc-pVDZ (vacuum). Grey areas show the possible range of conformations associated with the respective stereoinduction model for nucleophile addition to the carbonyl (PFA:  $285 \pm 5^\circ$ , *anti*-PFA:  $75 \pm 5^\circ$ , CE:  $165 \pm 15^\circ$ , *anti*-CE:  $195 \pm 15^\circ$ ).

bound, strongly electronegative heteroatom, like halogens and oxygen.<sup>[13,37,38]</sup> NMR-based conformational analysis of the simple oxirane-2-carbaldehyde ( $R^\alpha = R^\beta = R^{\beta'} = H$ ) showed such a *gauche/anti* orientation to be favored in solution as a result of dipole-dipole interactions with the carbonyl group.<sup>[39]</sup> In this early study the electron-withdrawing effect of epoxides was reported to be lower than for 2-alkoxy substituents. On the other hand, epoxides carry a considerable dipole moment of  $\mu \approx 1.9$  D (for oxirane),<sup>[37]</sup> comparable to fluoroethane ( $\mu = 1.94$  D)<sup>[40]</sup> and surpassing regular ethers ( $\mu = 1.3$  D for dimethyl ether, 1.63 D for THF). Hence, it was necessary to investigate whether the epoxide would primarily govern asymmetric induction according to the CE model or whether PFA-type stereoelectronics would significantly contribute to TS geometry.

Furthermore, ground state conformations alone cannot explain the variations in diastereoselectivity for the allylboration of differently substituted epoxy aldehydes (Scheme 6), as the rotational energy profiles were almost invariant to changes of the substitution pattern. To approach this issue, we initially applied the commonly used TS structural analysis to *trans* allylboration of general  $\alpha$ -heteroatom-substituted aldehydes which predicts a 2,3-*anti*-3,4-*anti* configuration in the product **A** for both stereoinduction models (Scheme 7A).<sup>[8b,13]</sup> Preference for either the PFA or the CE variant of **TS-A**<sub>trans</sub> would drastically depend on the size and electronegativity of the substituent X, also in comparison to the size and electronegativity of the second substituent R', calling for a computational in-depth analysis of the transition states.

For *cis* allylboration, the CE and PFA model each predict different product stereochemistry.<sup>[14b]</sup> In detail, a strongly electronegative  $\alpha$  substituent X should enforce a CE pathway [**TS-**

**B<sub>cis</sub>(CE)**], resulting in a 2,3-*anti*-3,4-*syn* configured product **A** (Scheme 7B). For less electronegative groups X a similar minimization of 1,3 *syn*-pentane interactions should be realized in the *anti*-PFA TS [**TS-B<sub>cis</sub>( $\alpha$ -PFA)**] leading to a 2,3-*syn*-3,4-*syn* stereochemistry.<sup>[13,14b,17]</sup> This divergent interplay between electrostatic, steric and hyperconjugative contributions could account for the poor stereocontrol sometimes found for allylboration of polar aldehydes.<sup>[14c,16a,28b,29]</sup>

To identify the factors influencing the stereoselectivity in the *cis* and *trans* allylboration of the epoxide-containing products **12/13 i <sup>$\alpha,\beta,\beta'$</sup>** , **12/13 j <sup>$\alpha,\beta,\beta'$</sup>** , **12/13 k <sup>$\alpha,\alpha',\beta$</sup>** , and **12/13 l <sup>$\alpha,\beta$</sup>** , a computational TS analysis of the allylboration of simplified versions of the experimentally used, differently substituted  $\alpha,\beta$ -epoxy aldehydes **14 d <sup>$\alpha,\beta,\beta'$</sup>** , **14 e <sup>$\alpha,\beta,\beta'$</sup>** , **14 f <sup>$\alpha,\alpha',\beta$</sup>** , and **14 g <sup>$\alpha,\beta$</sup>**  was conducted (for structural formulae see Figure SI-1). These model substrates **17 <sup>$\alpha,\beta,\beta'$</sup>** , **18 <sup>$\alpha,\alpha',\beta$</sup>** , and **19 <sup>$\alpha,\beta$</sup>**  display the three epoxy substitution patterns of interest as indicated by the respective superscript (for structural formulae see Figure 2) and should allow to deduce transferable trends about asymmetric induction mechanisms that led to the different diastereoselectivities.

The reaction partners, 2-(silyloxymethyl)allylboronates *cis*- and *trans*-**5**, were simplified to the 2-(methoxymethyl)allylboronates *trans*-**20** [Scheme 2. **D**, R<sup>*trans*</sup>=R<sup>2</sup>=Me, BX<sub>2</sub>=B(pin)] and *cis*-**20** [R<sup>*cis*</sup>=R<sup>2</sup>=Me, BX<sub>2</sub>=B(pin)], allowing for a reasonable computational model. Four cyclic, chair-like TS structures were generated as input for each of the three substrates,<sup>[14d,41]</sup> featuring an epoxide orientation associated with the respective model, being *anti* to the incoming nucleophile (PFA-type) or *anti* to the carbonyl group (CE-type). The resulting 24 possible structures were found to give stable TSs with activation energies in between  $\Delta G^\ddagger = 12\text{--}17\text{ kcal mol}^{-1}$  for *trans* and  $10\text{--}17\text{ kcal mol}^{-1}$  for *cis* allylboration. CE-type TSs proved to be energetically favored over PFA-type ones by  $0.9\text{--}4.4\text{ kcal mol}^{-1}$  for *trans* and  $0.72\text{--}2.99\text{ kcal mol}^{-1}$  for the *cis* allylboration, with the exception of aldehyde **18 <sup>$\alpha,\alpha',\beta$</sup>**  where the additional  $\alpha'$  substituent induced steric restrictions that render an *anti*-CE structure most stable with an energy gap of only  $0.28\text{ kcal mol}^{-1}$  to the corresponding *anti*-PFA TS.

The most stable TS for each *cis*- and *trans*-2-(methoxymethyl)allylboration of the three aldehydes is depicted in Figure 3. To rule out the relevance of other TS geometries, additional boat-like variants of the TSs were generated as input structures.<sup>[42]</sup> These proved to be unstable during the calculation and transformed into the corresponding chair-like structures. Indeed, previous computational studies on carbonyl allylboration found boat and twist-boat conformations to be  $4\text{--}8\text{ kcal mol}^{-1}$  higher in energy than their chair analogs, rendering them rather unimportant for this kind of reactions.<sup>[41]</sup>

In line with previous computational studies, all of the calculated structures represent an “early” TS regarding the C–C bond to be formed ( $d_{C-C} = 2.2\text{--}2.4\text{ \AA}$ ),<sup>[14d,35]</sup> show an attack trajectory angle within the Bürgi–Dunitz range of  $\alpha_{C-C-O} = 102\text{--}104^\circ$ ,<sup>[12,14d]</sup> and don't show a short distance between the methoxy oxygen atom and the aldehyde's hydrogen atom, previously reported as a strong TS geometry-defining interaction.<sup>[42]</sup> The relative energies ( $\Delta\Delta G^\ddagger$ ) of all calculated TSs are given in Table 1. A compilation of all TS structures including detailed

Structure	Allylboronate	Substrate	$\Delta\Delta G^\ddagger$ [kcal mol <sup>-1</sup> ]			
			PFA	CE	$\alpha$ -PFA	$\alpha$ -CE
<b>TS-1 t<sub>trans</sub></b>	<i>trans</i> - <b>20</b>	<b>17<sup><math>\alpha,\beta,\beta'</math></sup></b>	2.80	0	1.27	1.98
<b>TS-2 t<sub>trans</sub></b>	<i>trans</i> - <b>20</b>	<b>18<sup><math>\alpha,\alpha',\beta</math></sup></b>	4.41	0	0.88	3.26
<b>TS-3 t<sub>trans</sub></b>	<i>trans</i> - <b>20</b>	<b>19<sup><math>\alpha,\beta</math></sup></b>	2.12	0	2.35	1.06
<b>TS-4 c<sub>is</sub></b>	<i>cis</i> - <b>20</b>	<b>17<sup><math>\alpha,\beta,\beta'</math></sup></b>	2.99	0	0.72	0.80
<b>TS-5 c<sub>is</sub></b>	<i>cis</i> - <b>20</b>	<b>18<sup><math>\alpha,\alpha',\beta</math></sup></b>	3.87	2.66	0.28	0
<b>TS-6 c<sub>is</sub></b>	<i>cis</i> - <b>20</b>	<b>19<sup><math>\alpha,\beta</math></sup></b>	1.66	0	0.77	2.96

geometrical factors, bond dipole orientations, and critical steric interactions is given in Figures SI-3 and SI-4.

Overall, the DFT-computational TS analysis of epoxy aldehyde's *cis* and *trans* allylboration disclosed a similar preference for dipole moment minimization as already indicated by the rotational energy profiles in the ground state. Hence, electrostatics favored CE TS conformations with an *anti*-orientation of the former carbonyl group and the epoxide's C–O bond and thus O–C–C–O dihedral angles of  $153^\circ \leq \theta_{TS} \leq 179^\circ$  (Figures 2, SI-3, and SI-4). Besides missing dipole minimization, PFA-type TSs were additionally destabilized by *syn*-pentane and *gauche* interactions of the epoxide's substituents with the allylboronate's residue in position 3, R<sup>*trans*</sup> or R<sup>*cis*</sup>.

Regarding the stereochemical outcome of the allylboration, the most stable CE TS geometry would indeed lead to 2,3-*anti*-3,4-*anti* configuration in the product of *trans* allylboration and 2,3-*anti*-3,4-*syn* for the general *cis* allylboration, as well as 2,3-*syn*-3,4-*syn* for the special *cis* allylboration case toward  $\alpha$ -disubstituted product **12 k <sup>$\alpha,\alpha',\beta$</sup>** . These match the experimental findings shown in Scheme 6 and the theoretical analysis depicted in Scheme 7, again showing the strongly electronegative character of the epoxide group and the competitive effect of two  $\alpha$ -substituents with a similar level of asymmetric induction. Although structural simplifications had to be adopted for computational reasons, the calculated relative energies parallel the experimentally observed trend of diastereoselectivity being dependent on the epoxide's substitution pattern (Table 1). Hence, the  $\alpha,\beta,\beta'$  trisubstitution which showed a high level of stereoinduction in the experiments also features the biggest TS energy separation to the next opposite pathway in case of *trans* allylboration [**TS-1 t<sub>trans</sub>(CE)** vs. ( $\alpha$ -PFA)]. The differences were lower in energy for  $\alpha,\alpha',\beta$  (**TS-2 t<sub>trans</sub>**) and  $\alpha,\beta$ -*trans* substitution (**TS-3 t<sub>trans</sub>**; Figure 3, Scheme 6), in line with the experimental data. While a preference for CE-associated pathways was also found for *cis* allylboration, the computational model cannot fully explain the high diastereoselectivity just found for  $\alpha,\beta,\beta'$  trisubstitution. This is probably due to the truncation of the side chains and the substitution of the bulky OSiMe<sub>2</sub>tBu for the small OCH<sub>3</sub> group in the computational model, known to drastically influence TS geometries in related boron-enolate aldol reactions,<sup>[42]</sup> as well as the neglected solvent influence.

A comparison of the in silico generated TS structures disclosed three factors determining the energy differences in the TSs, correlating with the experimentally observed stereocontrol: (1) minimization of the dipole moment, (2) destabilizing *syn*-pentane and *gauche* interactions in PFA-type structures,



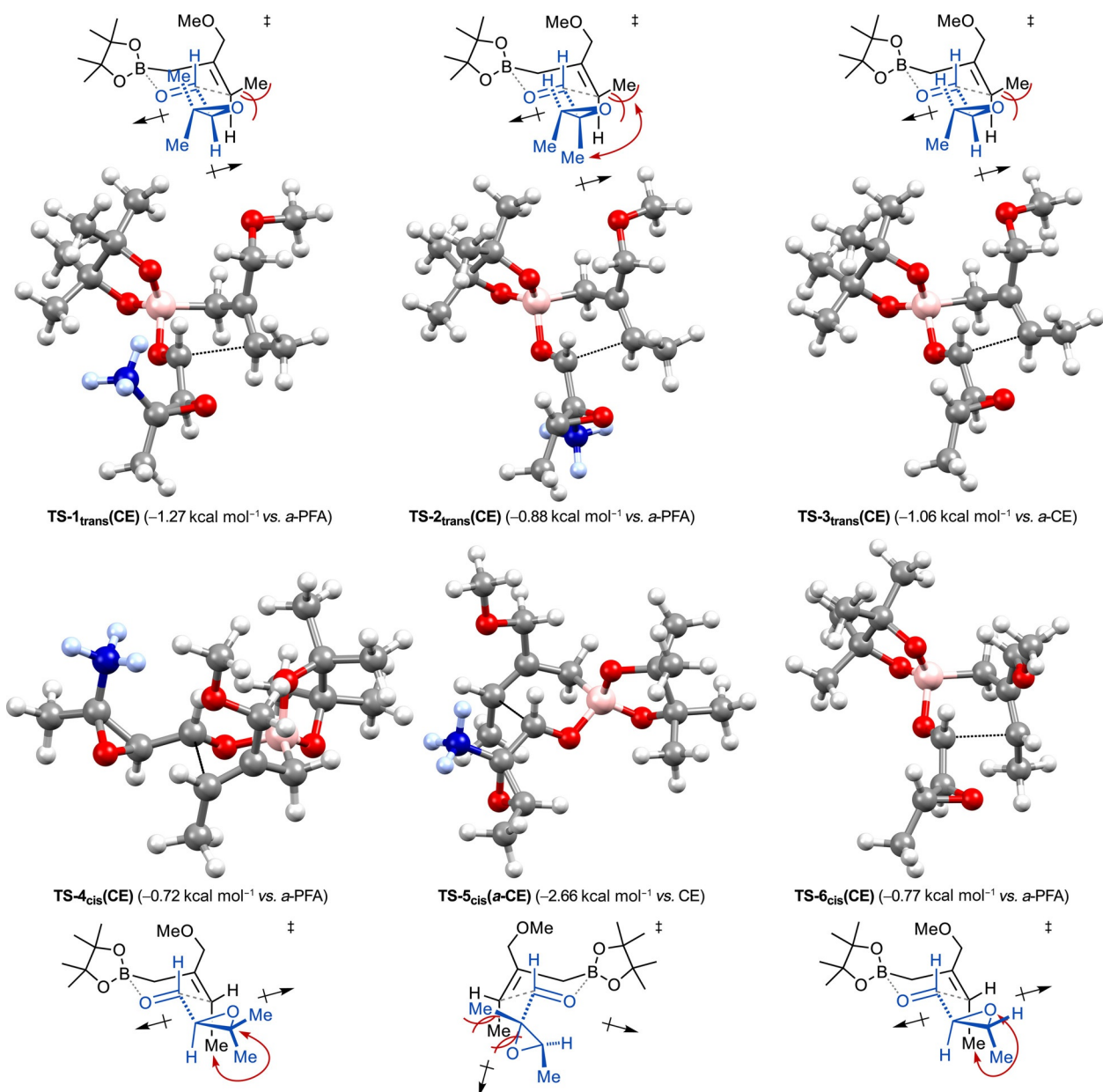


**Figure 3.** Transition state analysis by DFT calculation: Global minima for *cis* and *trans* allylboronate  $\alpha,\beta$ -epoxy aldehydes  $17^{\alpha,\beta,\beta'}$ ,  $18^{\alpha,\alpha',\beta}$ , and  $19^{\alpha,\beta}$ . Calculated at the B3LYP-D3(BJ)/cc-pVDZ level of theory (vacuum). The subscript *trans* or *cis* corresponds to the allylboronate geometry. The assignment to the respective stereinduction model is shown in bold parentheses. The energy difference ( $\Delta\Delta G^\ddagger$ ) to the next higher opposite TS (*pro* vs. *anti*, abbreviated as *a*) is given in light parentheses. The epoxy aldehyde's methyl group probe is highlighted in blue.

and (3) strong 1,3-asymmetric induction caused by steric repulsion with the substituent  $R^{\beta'}$ , if present (Figure 4).

As clearly shown by the calculations, electrostatics enforced a stabilizing *anti* orientation of the carbonyl group and the epoxide's C–O bond in the allylboronate of  $\alpha,\beta$ -epoxy aldehydes. The level of this effect can be qualitatively deduced from the *trans* and *cis* allylboronate of  $\alpha,\beta$ -disubstituted aldehyde substrate  $19^{\alpha,\beta}$  which shows a comparable level of rather weak repulsive steric interactions in all four TSs (CE, *anti*-CE, PFA, *anti*-PFA). For both allylboronate cases, being **TS-3<sub>trans</sub>** and **TS-6<sub>cis</sub>**, non-dipole minimized PFA-type states are disfavored by 0.8–2.4 kcal mol<sup>-1</sup>.

A comparison of all resulting TSs suggests that a high level of dipole moment-minimization can be realized in the CE cases ( $153^\circ \leq \theta_{TS} \leq 179^\circ$ ), but is significantly lowered in the *anti*-CE cases due to repelling interactions of the epoxide with the allylboronate substituent in position 3,  $R^{trans}$  or  $R^{cis}$ . This resulted in destabilization of *anti*-CE states with dihedral angles drastically differing from a  $(-180^\circ)$  maximum, being  $-42^\circ \geq \theta_{TS} \geq -60^\circ$  for *trans* and only  $-30^\circ \geq \theta_{TS} \geq -32^\circ$  for *cis* allylboronate (Figures 4, SI-3, and SI-4). The reduced stabilization of *anti*-CE TSs could account for the energetic similarity with *anti*-PFA TSs in some cases, which showed more favorable dihedral angles in the range of  $94^\circ \leq \theta_{TS} \leq 118^\circ$  (**TS-4<sub>cis</sub>**, **TS-5<sub>cis</sub>**).

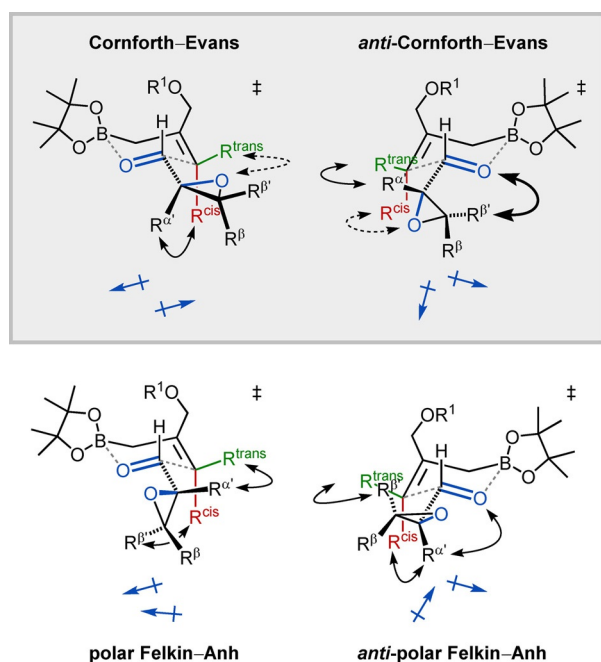


**Figure 4.** Rationale for stereocontrolled allylboration of  $\alpha,\beta$ -epoxy aldehydes according to the Cornforth–Evans model.

The distinct energetic differentiation between the four TSs in the reaction with  $\alpha,\beta,\beta'$ -trisubstituted epoxy aldehyde **17** <sup>$\alpha,\beta,\beta'$</sup>  resulted from a highly destabilizing allylic 1,3-strain between the substituent  $R^{\beta'}$  and the carbonyl oxygen in case of the *anti*-CE, or *syn*-pentane/*gauche* strain with the allylboronate's residue  $R^{\text{trans}}$  in the *anti*-PFA or  $R^{\text{cis}}$  in the PFA case (Figures 4 and SI-3). This combination of dipole minimization and 1,3-asymmetric induction by the residue  $R^{\beta'}$  is missing for the allylboration of epoxy aldehydes **18** <sup>$\alpha,\alpha',\beta$</sup>  and **19** <sup>$\alpha,\beta$</sup> , likely compromising stereoselectivity. For aldehyde **18** <sup>$\alpha,\alpha',\beta$</sup>  it is even counteracted by a non-productive *syn*-pentane strain in both CE-type TSs, caused by the substituent  $R^{\alpha'}$ . In this particular case the steric influence on the discrimination of “*pro*” and *anti*”-pathways seems to be slightly higher than the electrostatic effect of the sterically unimposing epoxy group. This led to a switch in stereochemistry as also found by experiment. The competition between similarly bulky or electronegative geminal  $\alpha$ -substituents on asymmetric induction has been described as a limiting factor of these stereochemical models (see Scheme 7B, X vs. R').<sup>[8b,13,14b,d,16b,c]</sup> In this case, it is the formal interplay between an electronegative oxygen atom and a considerably more bulky  $\text{CH}_3$  group. The computational overestimation of this effect for *cis* allylboration transition states is likely caused by simplifications adopted for the calculations regarding the chemical structures and computational methods.

## Conclusions

Functionalized 2-(silyloxymethyl)allylboronates were designed that combine chemical stability and predictable transfer of stereochemistry into allylboration products. They smoothly react with aldehydes without (Lewis) acid activation.<sup>[27]</sup> The general

*trans*- and *cis*-selective synthesis to this reagent class featured a late-stage construction of the allylboronate by using either a Negishi coupling or organomagnesium chemistry.

While the reaction of these reagents with  $\alpha$ -carbamato aldehydes proceeded according to the polar Felkin–Anh (PFA) model, more electronegative  $\alpha$ -alkoxy, especially  $\alpha,\beta$ -epoxy aldehydes, conformed to Cornforth–Evans (CE) stereoreduction. Hence, dipole moment-minimization in the transition state (TS) of allylboration is a strong directing force, as seen for aldol<sup>[14b,43]</sup> and Wittig reactions.<sup>[44]</sup> For simple nucleophiles both the PFA and the CE model predict the same product stereochemistry. This degeneracy was resolved by *cis* allylboration that led to a distinct product fitting to the CE model. The level of stereocontrol for the allylboration of  $\alpha,\beta$ -epoxy aldehydes was found to be strongly dependent on epoxide substitution, with a  $\beta$ -*cis* substitution leading to constantly high diastereoselectivity by the combination of dipole minimization and 1,3 asymmetric induction.  $\alpha,\alpha$ -Di-substitution was found to impede viable asymmetric induction by contributing additional steric interactions that compete with dipole minimization.

DFT analysis of the ground state conformations of differently substituted  $\alpha,\beta$ -epoxy aldehydes and the possible allylboration TSs verified the preference of dipole-minimizing conformations. Hyperconjugative stabilization according to the PFA model clearly seemed overridden by electrostatics in case of  $\alpha,\beta$ -epoxy aldehydes, classifying epoxides as “strongly electronegative”  $\alpha$ -substituents.<sup>[13]</sup> Additionally, the experimentally observed dependence of stereocontrol on an epoxide's  $\beta$ -*cis* substituent was identified by computation as a selector for the CE transition state. This substitution reinforces the otherwise weak facial discrimination of the carbonyl group in the CE transition state by the apparently well ordered, but spatially unimposing epoxide group.

By applying this rationale in a forward sense,  $\alpha,\beta$ -epoxy aldehydes and allylboronates can now be readily applied for the stereocontrolled synthesis of complex polyhydroxylated target molecules. Further investigations notwithstanding, it is expected that the consistent results obtained herein will apply to most addition reactions to epoxy aldehydes. Overall, Cornforth–Evans transition states and the impact of dipole minimization should always be considered for addition reactions to carbonyl compounds.

## Experimental Section

Detailed descriptions of instrumentation, materials, experimental procedures, product characterization (1D and 2D NMR including copies of spectra, HRMS, IR, optical rotation), computational details and primary data, as well as a list of abbreviations is given in the Supporting Information.

### General procedure M1 for 2-(silyloxymethyl)allylboronate synthesis by using Grignard chemistry

A solution of a substituted vinyl iodide (1.0 equiv) in anhydrous  $\text{Et}_2\text{O}$  (0.3 M in substrate) was added dropwise to a stirred solution of (alkoxide- and hydroxide-free) *t*BuLi (2.0 equiv, 1.9 M in pentane) in anhydrous  $\text{Et}_2\text{O}$  (0.3 M in *t*BuLi) at  $-78^\circ\text{C}$ . A freshly prepared an-

hydrous  $\text{MgBr}_2 \cdot \text{OEt}_2$  solution (1.0 equiv, 0.8 M in 4:1  $\text{Et}_2\text{O}/\text{C}_6\text{H}_6$ ) was added after 2 h at this temperature (TLC control). After an additional hour at  $-78^\circ\text{C}$  a solution of anhydrous  $\text{ICH}_2\text{B}(\text{pin})$  (1.1 equiv, dehydrated by passing through a plug of activated neutral  $\text{Al}_2\text{O}_3$  directly before use) in anhydrous  $\text{Et}_2\text{O}$  (0.7 M in reagent) was slowly added via the cooled inner wall of the reaction vessel. The resulting suspension was allowed to slowly warm to  $-20^\circ\text{C}$  and kept at this temperature for 15 h. The cooling bath was removed and the mixture was added to stirred phosphate buffer (pH 6, 0.5 M, ca. 10 mL per mmol of substrate) at  $0^\circ\text{C}$ . The mixture was extracted with MTBE (ca. 20 mL per mmol substrate) and the extract was washed with brine (ca. 10 mL per mmol substrate). The organic extract was dried with  $\text{MgSO}_4$ , filtered, and the solvent was removed in vacuo at  $25^\circ\text{C}$ . Rapid (5–10 min) silica gel column chromatography of the residue ( $3 \times 10$  cm for 0.6 mmol substrate) provided allylboronate **5**.

#### General procedure M2 for 2-(silyloxymethyl)allylboronate synthesis by using Negishi couplings

To a stirred solution of  $[\text{Pd}(\text{PPh}_3)_4]$  (0.1 equiv) in anhydrous, deoxygenated THF (ca. 0.02 M in Pd catalyst) at  $20^\circ\text{C}$  was added a solution of  $\text{IZnCH}_2\text{B}(\text{pin})$  (2.0 equiv, 0.6 M in anhydrous THF), followed by a solution of a substituted vinyl iodide (1.0 equiv) in anhydrous THF (ca. 0.25 M in substrate). The flask was immersed in a preheated  $60^\circ\text{C}$  oil bath and the mixture was stirred for 3 h (GC-MS control). The oil bath was removed and the mixture was cooled to  $0^\circ\text{C}$  whereupon it was added to stirred phosphate buffer (pH 6, 0.5 M, ca. 30 mL per mmol of substrate) at  $0^\circ\text{C}$ . After complete addition, the mixture was extracted with MTBE ( $\approx 30$  mL per mmol of substrate) and the extract was washed with brine (ca. 30 mL per mmol substrate). The organic extract was dried with  $\text{MgSO}_4$ , filtered, and the solvent was removed in vacuo at  $25^\circ\text{C}$ . Rapid (10 min) silica gel column chromatography of the residue ( $4 \times 10$  cm for 2.4 mmol substrate) provided allylboronate **5**.

#### General procedure (a) for 2-(silyloxymethyl)allylboration of aldehydes

Allylboronate **5** (1.0 equiv) was added to a stirred solution of aldehyde **11/14** (1.1 equiv) in anhydrous  $\text{Et}_2\text{O}$  (0.15 M in boronate) at  $0^\circ\text{C}$ . The solution was allowed to reach  $20^\circ\text{C}$  over 4 h. After 24 h at this temperature (TLC control) the solution was directly subjected to silica gel column chromatography ( $1.5 \times 25$  cm for  $\approx 0.05$  mmol of substrate) to obtain the homoallylic alcohol product **12/13**.

#### General procedure (b) for 2-(silyloxymethyl)allylboration of aldehydes

Allylboronate **5** (1.0 equiv) was added to a stirred suspension of aldehyde **11/14** (1.1 equiv) and  $\text{NaHCO}_3$  (0.30 mg,  $3.55 \mu\text{mol}$ , 0.05 equiv) in anhydrous  $\text{Et}_2\text{O}$  (0.5 mL) at  $0^\circ\text{C}$ . The mixture was kept at this temperature for 48 h (TLC control) whereupon it was directly subjected to silica gel column chromatography ( $1.5 \times 25$  cm for ca. 0.05 mmol of substrate) to obtain the homoallylic alcohol product **12/13**. Alternative workup for larger scale: Sat.  $\text{NaHCO}_3$  solution ( $\approx 9$  mL per mmol of substrate) was added and the biphasic mixture was stirred for 5 min. The organic layer was separated and washed with brine ( $\approx 9$  mL per mmol substrate). The organic extract was dried with  $\text{MgSO}_4$ , filtered, and the solvent was removed in vacuo at  $25^\circ\text{C}$ . The homoallylic alcohol **12/13** was obtained after silica gel column chromatography ( $3 \times 20$  cm for 2.2 mmol boronate) of the residue.

#### General procedure for the preparation of oxazolidinones SI-1/SI-2/SI-3 from *N*-Boc $\alpha$ -amino alcohols

To a stirred solution of *N*-Boc  $\alpha$ -amino alcohol **12 f/13 f** (1.0 equiv) in anhydrous THF (0.07 M in substrate) at  $0^\circ\text{C}$  was added NaH (2.0 equiv, 60 weight% in mineral oil) in one portion. The suspension was allowed to warm to  $20^\circ\text{C}$  during 2 h and stirred at this temperature for 14 h (TLC control). The mixture was diluted with MTBE ( $\approx 3.8$  mL per  $10 \mu\text{mol}$  of substrate) and sat.  $\text{NH}_4\text{Cl}$  solution (ca. 3.8 mL per  $10 \mu\text{mol}$  of substrate). The organic layer was then separated and washed with brine (ca. 3.8 mL per  $10 \mu\text{mol}$  substrate). The organic extract was dried with  $\text{MgSO}_4$ , filtered, and the solvent was removed in vacuo. Silica gel column chromatography ( $2 \times 15$  cm for 0.04 mmol of substrate) of the residue delivered the oxazolidinone **SI-1/SI-2/SI-3**.

#### General procedure for the preparation of Mosher esters SI-6/SI-7/SI-8 from secondary alcohols

To a solution of a secondary alcohol (1.0 equiv) and DMAP (4.0 equiv) in anhydrous THF (0.04 M in substrate) was added (*R*)-(–)-MTPA-Cl (1.0–1.6 equiv) at  $0^\circ\text{C}$  with stirring. The cooling bath was removed after 10 min and the suspension was allowed to warm to  $20^\circ\text{C}$ . After 16 h at this temperature (TLC control) MTBE ( $\approx 1.8$  mL per  $10 \mu\text{mol}$  of substrate) and sat.  $\text{NaHCO}_3$  solution (ca. 0.6 mL per  $10 \mu\text{mol}$  of substrate) were added to the suspension. After additional 10 min of stirring, the mixture was added to MTBE (ca. 6 mL per  $10 \mu\text{mol}$  of substrate) and sat.  $\text{NaHCO}_3$  solution (ca. 6 mL per  $10 \mu\text{mol}$  of substrate). The organic layer was separated, washed with sat.  $\text{NaHCO}_3$  solution (ca. 6 mL per  $10 \mu\text{mol}$  of substrate), and brine (ca. 6 mL per  $10 \mu\text{mol}$  of substrate), dried with  $\text{MgSO}_4$ , filtered, and concentrated in vacuo at  $25^\circ\text{C}$ . Silica gel column chromatography of the residue ( $\text{SiO}_2$  15–40  $\mu\text{m}$ ,  $1.5 \times 15$  cm for ca. 16  $\mu\text{mol}$  of substrate) provided the (*S*)-MTPA ester (**S**)-**SI-6/SI-7/SI-8**. The (*R*)-MTPA ester (*R*)-**SI-6/SI-7/SI-8** were analogously prepared from the epoxy alcohol using (*S*)-(+)-MTPA-Cl.

#### Computational details

All spin polarized density functional theory (DFT) calculations were performed within the Orca program package version 4.0.1,<sup>[45]</sup> whereas input structures for transition state geometry optimization were generated with the Spartan 14v114 software by the semi-empirical parameterized model 6 (PM6) method.<sup>[46]</sup> For all DFT calculations the correlation consistent cc-pVDZ basis set according to Dunning was used.<sup>[36d]</sup> The exchange and correlation effects were taken into account with the hybrid functional by Becke and Lee–Yang–Parr (B3LYP)<sup>[36c,e]</sup> and dispersion interactions were considered via the Becke–Johnson damping Scheme [D3(BJ)].<sup>[36a,b]</sup> For the energy rotation profiles, constrained geometry optimizations were performed at fixed dihedral angles, which were spanned by the oxygen atom of the respective epoxide and aldehyde groups. The transition states were located by calculating the Hesse matrix and fully optimizing their geometries in the gas phase. By calculating the vibrational frequencies within the harmonic approximation, the optimized structures were confirmed as transition states through the presence of only one imaginary frequency.

#### Acknowledgements

Partial support by the *TMWWDG* (grant no. 43–5572–321–12040–12, to H.-D. A) and the *DFG* (SFB 1127, to H.-D. A.) is acknowledged. R. R. A. F. was a recipient of a doctoral fellowship

from the *Fonds der Chemischen Industrie* (FCI). Computational resources were provided by the state of *Baden-Württemberg* through bwHPC and the *DFG* (INST 40/467-1 FUGG, to T. J.).

## Conflict of interest

The authors declare no conflict of interest.

**Keywords:** allylation · allylboronates · Cornforth–Evans · stereoreduction models · synthetic methods

- [1] a) P. A. Frey, A. D. Hegeman, *Enzymatic reaction mechanisms*, Oxford University Press, 2007; b) M. E. Glasner, J. A. Gerlt, P. C. Babbitt, *Curr. Opin. Chem. Biol.* **2006**, *10*, 492–497.
- [2] a) R. B. Woodward, E. Logusch, K. P. Nambiar, K. Sakan, D. E. Ward, B. W. Au-Yeung, P. Balaram, L. J. Browne, P. J. Card, C. H. Chen, *J. Am. Chem. Soc.* **1981**, *103*, 3210–3213; b) H. Nagaoka, Y. Kishi, *Tetrahedron* **1981**, *37*, 3873–3888.
- [3] J.-D. Zhai, D. Li, J. Long, H.-L. Zhang, J.-P. Lin, C.-J. Qiu, Q. Zhang, Y. Chen, *J. Org. Chem.* **2012**, *77*, 7103–7107.
- [4] S. Roscales, J. Plumet, *Int. J. Carbohydr. Chem.* **2016**, Article ID 4760548.
- [5] W.-J. Chung, J. S. Carlson, D. K. Bedke, C. D. Vanderwal, *Angew. Chem. Int. Ed.* **2013**, *52*, 10052–10055; *Angew. Chem.* **2013**, *125*, 10236–10239.
- [6] a) T. Sawano, H. Yamamoto, *J. Org. Chem.* **2018**, *83*, 4889–4904; b) A. M. Bailey, S. Wolfrum, E. M. Carreira, *Angew. Chem. Int. Ed.* **2016**, *55*, 639–643; *Angew. Chem.* **2016**, *128*, 649–653; c) Q. Wu, C. Wu, H. Long, R. Chen, D. Liu, P. Proksch, P. Guo, W. Lin, *J. Nat. Prod.* **2015**, *78*, 2461–2470; d) M. Sasaki, K. Tanino, A. Hirai, M. Miyashita, *Org. Lett.* **2003**, *5*, 1789–1791; e) R. M. Hanson, *Chem. Rev.* **1991**, *91*, 437–475.
- [7] R. R. A. Freund, P. Gobrecht, Z. Rao, J. Gerstmeier, R. Schlosser, H. Görls, O. Werz, D. Fischer, H.-D. Arndt, *Chem. Sci.* **2019**, *10*, 7358–7364.
- [8] a) T.-P. Loh, Z. Yin, H.-Y. Song, K.-L. Tan, *Tetrahedron Lett.* **2003**, *44*, 911–914; b) A. Mengel, O. Reiser, *Chem. Rev.* **1999**, *99*, 1191–1223; c) M. J. Wanner, N. P. Willard, G. J. Koomen, U. K. Pandit, *Tetrahedron* **1987**, *43*, 2549–2556; d) R. H. Schlessinger, J. L. Wood, *J. Org. Chem.* **1986**, *51*, 2621–2623; e) D. A. Hutchison, K. R. Beck, R. A. Benkeser, J. B. Grutzner, *J. Am. Chem. Soc.* **1973**, *95*, 7075–7082.
- [9] A. D. Walsh, *Trans. Faraday Soc.* **1949**, *45*, 179–190.
- [10] a) N. Bartlett, L. Gross, F. Péron, D. J. Asby, M. D. Selby, A. Tavassoli, B. Linclau, *Chem. Eur. J.* **2014**, *20*, 3306–3310; b) F. Zhang, Y. Liu, L. Xie, X. Xu, *RSC Adv.* **2014**, *4*, 17218–17221; c) Y. Takeda, T. Matsumoto, F. Sato, *J. Org. Chem.* **1986**, *51*, 4728–4731; d) L. A. Paquette, T. M. Mitzel, *J. Am. Chem. Soc.* **1996**, *118*, 1931–1937.
- [11] a) N. T. Anh, O. Eisenstein, *Nouv. J. Chim.* **1977**, *1*, 61–70; b) M. Chérest, H. Felkin, N. Prudent, *Tetrahedron Lett.* **1968**, *9*, 2199–2204.
- [12] a) H. B. Bürgi, J. D. Dunitz, J. M. Lehn, G. Wipff, *Tetrahedron* **1974**, *30*, 1563–1572; b) H. B. Bürgi, J. D. Dunitz, E. Shefter, *J. Am. Chem. Soc.* **1973**, *95*, 5065–5067.
- [13] V. J. Cee, C. J. Cramer, D. A. Evans, *J. Am. Chem. Soc.* **2006**, *128*, 2920–2930.
- [14] a) R. E. Rosenberg, W. J. Kelly, *J. Phys. Org. Chem.* **2015**, *28*, 47–56; b) D. A. Evans, S. J. Siska, V. J. Cee, *Angew. Chem. Int. Ed.* **2003**, *42*, 1761–1765; *Angew. Chem.* **2003**, *115*, 1803–1807; c) J. A. Marco, M. Carda, S. Díaz-Oltra, J. Murga, E. Falomir, H. Roeper, *J. Org. Chem.* **2003**, *68*, 8577–8582; d) B. W. Gung, X. Xue, *Tetrahedron: Asymmetry* **2001**, *12*, 2955–2959; e) W. R. Roush, M. A. Adam, A. E. Walts, D. J. Harris, *J. Am. Chem. Soc.* **1986**, *108*, 3422–3434.
- [15] J. W. Cornforth, R. H. Cornforth, K. K. J. Mathew, *J. Chem. Soc.* **1959**, 112–127.
- [16] a) C. Gennari, E. Fioravanzo, A. Bernardi, A. Vulpetti, *Tetrahedron* **1994**, *50*, 8815–8826; b) C. Gennari, S. Vieth, A. Comotti, A. Vulpetti, J. M. Goodman, I. Paterson, *Tetrahedron* **1992**, *48*, 4439–4458; c) W. R. Roush, *J. Org. Chem.* **1991**, *56*, 4151–4157.
- [17] I. Fleming, *Molecular Orbitals and Organic Chemical Reactions: Reference Edition*, John Wiley & Sons, **2010**, 226–229.
- [18] a) Y. Zhang, Y. Wu, *Org. Biomol. Chem.* **2010**, *8*, 4744–4752; b) A. Alexakis, P. Mangeney, J. F. Normant, *Tetrahedron Lett.* **1985**, *26*, 4197–4200.
- [19] H. Ren, A. Krasovskiy, P. Knochel, *Chem. Commun.* **2005**, 543–545.
- [20] A. Krasovskiy, B. F. Straub, P. Knochel, *Angew. Chem. Int. Ed.* **2006**, *45*, 159–162; *Angew. Chem.* **2006**, *118*, 165–169.
- [21] K. Kitagawa, A. Inoue, H. Shinokubo, K. Oshima, *Angew. Chem. Int. Ed.* **2000**, *39*, 2481–2483; *Angew. Chem.* **2000**, *112*, 2594–2596.
- [22] a) R. W. Hoffmann, T. Sander, A. Hense, *Liebigs Ann. Chem.* **1993**, 771–775; b) T. Watanabe, N. Miyaara, A. Suzuki, *J. Organomet. Chem.* **1993**, *444*, C1–C3; c) P. Knochel, *J. Am. Chem. Soc.* **1990**, *112*, 7431–7433.
- [23] D. F. Taber, M. I. Sikkander, J. F. Berry, K. J. Frankowski, *J. Org. Chem.* **2008**, *73*, 1605–1607.
- [24] A. Yanagisawa, S. Habaue, H. Yamamoto, *J. Am. Chem. Soc.* **1991**, *113*, 5893–5895.
- [25] I. W. Ashworth, J. A. L. Miles, D. J. Nelson, J. M. Percy, K. Singh, *Tetrahedron* **2009**, *65*, 9637–9646.
- [26] R. R. A. Freund, P. Gobrecht, P. Moser, D. Fischer, H.-D. Arndt, *Org. Biomol. Chem.* **2019**, *17*, 9703–9707.
- [27] T. G. Elford, D. G. Hall, *Synthesis* **2010**, 893–907.
- [28] a) P. G. M. Wuts, S. S. Bigelow, *J. Org. Chem.* **1988**, *53*, 5023–5034; b) W. R. Roush, M. A. Adam, D. J. Harris, *J. Org. Chem.* **1985**, *50*, 2000–2003.
- [29] G. Niel, F. Roux, Y. Maisonnasse, I. Maugras, J. Poncet, P. Jouin, *J. Chem. Soc. Perkin Trans. 1* **1994**, 1275–1280.
- [30] T. R. Hoye, C. S. Jeffrey, F. Shao, *Nat. Protoc.* **2007**, *2*, 2451–2458.
- [31] M. Chen, W. R. Roush, *J. Am. Chem. Soc.* **2012**, *134*, 3925–3931.
- [32] A. Ghantous, H. Gali-Muhtasib, H. Vuorela, N. A. Saliba, N. Darwiche, *Drug Discovery Today* **2010**, *15*, 668–678.
- [33] T. M. Hansen, G. F. Florence, P. Lugo-Mas, J. Chen, J. N. Abrams, C. J. Forsyth, *Tetrahedron Lett.* **2003**, *44*, 57–59.
- [34] a) R. Bloch, C. Brillet, *Synlett* **1991**, 829–830; b) R. R. A. Freund, H.-D. Arndt, *J. Org. Chem.* **2016**, *81*, 11009–11016.
- [35] J. J. Gajewski, W. Bocian, N. L. Brichford, J. L. Henderson, *J. Org. Chem.* **2002**, *67*, 4236–4240.
- [36] a) S. Grimme, S. Ehrlich, L. Goerigk, *J. Comput. Chem.* **2011**, *32*, 1456–1465; b) S. Grimme, J. Antony, S. Ehrlich, H. Krieg, *J. Chem. Phys.* **2010**, *132*, 154104; c) A. D. Becke, *J. Chem. Phys.* **1993**, *98*, 5648–5652; d) T. H. Dunning, Jr., *J. Chem. Phys.* **1989**, *90*, 1007–1023; e) C. Lee, W. Yang, R. G. Parr, *Phys. Rev. B* **1988**, *37*, 785–789.
- [37] R. M. Pontes, B. C. Fiorin, E. A. Basso, *Chem. Phys. Lett.* **2004**, *395*, 205–209.
- [38] G. Frenking, K. F. Köhler, M. T. Reetz, *Tetrahedron* **1993**, *49*, 3971–3982.
- [39] G. J. Karabatsos, D. J. Fenoglio, *J. Am. Chem. Soc.* **1969**, *91*, 3577–3582.
- [40] W. M. Haynes, *CRC Handbook of Chemistry and Physics*, 97 ed., CRC press, **2017**, 9–59–59-67.
- [41] a) A. Vulpetti, M. Gardner, C. Gennari, A. Bernardi, J. M. Goodman, I. Paterson, *J. Org. Chem.* **1993**, *58*, 1711–1718; b) Y. Li, K. N. Houk, *J. Am. Chem. Soc.* **1989**, *111*, 1236–1240.
- [42] R. S. Paton, J. M. Goodman, *J. Org. Chem.* **2008**, *73*, 1253–1263.
- [43] S. E. Denmark, G. L. Beutner, T. Wynn, M. D. Eastgate, *J. Am. Chem. Soc.* **2005**, *127*, 3774–3789.
- [44] R. Robiette, J. Richardson, V. K. Aggarwal, J. N. Harvey, *J. Am. Chem. Soc.* **2005**, *127*, 13468–13469.
- [45] F. Neese, *Wiley Interdiscip. Rev.: Comput. Mol. Sci.* **2012**, *2*, 73–78.
- [46] a) J. J. P. Stewart, *J. Mol. Model.* **2007**, *13*, 1173–1213; b) *Spartan “14*, Irvine, **2014**.

Manuscript received: March 27, 2020

Revised manuscript received: April 1, 2020

Accepted manuscript online: April 2, 2020

Version of record online: June 22, 2020